Electric Power Systems Research 218 (2023) 109195

Contents lists available at ScienceDirect

Electric Power Systems Research

journal homepage: www.elsevier.com/locate/epsr

Multi-objective stochastic techno-economic-environmental optimization of distribution networks with G2V and V2G systems

Seyed Ehsan Ahmadi [a], S. Mahdi Kazemi-Razi [a], Mousa Marzband [a,b,*], Augustine Ikpehai [c], Abdullah Abusorrah [b,d]

[a] Northumbria University, Electrical Power and Control Systems Research Group, Ellison Place NE1 8ST, Newcastle upon Tyne, UK
[b] Center of Research Excellence in Renewable Energy and Power Systems, King Abdulaziz University, Jeddah, 21589, Saudi Arabia
[c] Department of Engineering and Mathematics, Sheffield Hallam University, Sheffield S1 1WB, UK
[d] Department of Electrical and Computer Engineering, Faculty of Engineering, K. A. CARE Energy Research and Innovation Center, King Abdulaziz University, Jeddah 21589, Saudi Arabia

ARTICLE INFO

Keywords:
Plug-in electric vehicle
CO_2 emission
Firefly algorithm
Multi-objective optimization

ABSTRACT

Plug-in electric vehicles (PEVs) are one of the most promising technologies for decarbonizing the transportation sector towards the global Net-zero target. However, charging/discharging of PEVs impacts the electricity network's stability, increases the operating costs, and affects the voltage profile. This paper proposes a flexible multi-objective optimization approach to evaluate and deploy vehicle-to-grid and grid-to-vehicle technologies considering techno-economical and environmental factors. Furthermore, life cycle of PEV batteries, charging/discharging pattern, and driving behaviours of the PEV owners are considered. The simulations are run over a modified IEEE 69-bus radial distribution test system to minimize two objective functions including the operating costs and CO_2 emissions using the heuristic-based Firefly Algorithm in a stochastic optimization framework considering renewable generations, load consumption, and charging/discharging timing of PEVs as the uncertain parameters. The results demonstrate significant reductions in the operating costs and CO_2 emissions, and the voltage profile of the network is improved properly. Besides, by implementing the discharging facility of PEVs in the network, the PEV owners save a considerable amount in operating costs.

1. Introduction

1.1. Motivation

In recent times, there has been a growing awareness of the adverse effects of climate change. In a contemporary report from the United Nations (UN), climate change was declared a "code red for humanity" by the UN secretary-general [1]. Conversely, scientific researchers have shown that long term sustainable reductions in CO_2 and other greenhouse gases (GHG) emissions could improve air quality and stabilize global temperatures in 20 to 30 years [2]. However, the growing population and expanding industrial development pose a considerable challenge in decarbonizing the distribution networks (DNs) [3]. Hence, over the next two decades, the amount of electricity consumed is projected to rise by almost 50%, putting additional strain on existing power networks [4]. Furthermore, there are concerns about energy security, supply and fossil fuel's environmental and human impacts within the transportation system. To this end, plug-in electric vehicles (PEVs) are highly recommended as a practical solution to reduce the dependency on fossil fuels and decarbonizing the transportation sector [5]. Also, curbing air pollution from fossil fuel engines in the transportation system have necessitated the use of sustainable and renewable energy sources (RES), which has further increased the use of PEVs and RESs in DNs [6,7]. However, PEVs' integration into the electrical power grids causes significant technical, economic, and regulatory issues. Also, the increasing use of PEVs further constitutes more financial and decarbonization challenges in the operation of power and energy networks [8]. The environmental benefits of PEVs may differ subject to the combination of charging and driving patterns, weather condition, and the carbon intensity of the network [9]. However, most governments outline incentives to attain adoption objectives, only emphasizing on the number and type of PEV adopted as a result in contrast to the charging behaviour or the supporting RES capacity to balance extra PEV demand [10]. Furthermore, several regulations meant to motivate PEV owners have weakened carbon accounting by applying sales-averaged CO2 emissions that are reduced via PEV policy incentives and excluding charging emissions [11].

* Corresponding author.
E-mail address: mousa.marzband@northumbria.ac.uk (M. Marzband).

https://doi.org/10.1016/j.epsr.2023.109195
Received 18 October 2022; Received in revised form 28 December 2022; Accepted 5 February 2023
Available online 14 February 2023

Nomenclature

Acronyms

CP	Charging Point
DER	Distributed Energy Resource
DG	Distributed Generation
DN	Distribution Network
FA	Firefly Algorithm
FC	Fuel Cell
G2V	Grid to Vehicle
LHS	Latin Hypercube Sampling
MT	Micro-Turbine
MO	Multi-Objective
PV	Photovoltaic
PEV	Plug-in Electric Vehicle
RES	Renewable Energy Sources
STC	Standard Testing Condition
SOC	State of Charge
V2G	Vehicle to Grid
WT	Wind Turbine

Indices

c	Set for FC
g	Set for MT
b	Set for PEV
e	Set for renewable unit
l	Set for bus
s	Set for scenario
h	Set for time

Parameters

$P_{l,h}^{load}$	Active load in bus lth at hour h [kW]
$Q_{l,h}^{load}$	Reactive load in bus lth at hour h [kW]
P_{stc}^{pv}	Active power generated by a PV under standard testing condition [kW]
G^{pv}	Radiation intensity [kW/m^2]
G_{stc}^{pv}	Intensity of radiation under standard testing condition [kW/m^2]
$\lambda_{\text{mpt}}^{pv}$	Heat factor relating to the maximum power
T_c^{pv}	Temperature of PV module
T_{ref}^{pv}	Reference temperature
T_a^{pv}	Ambient temperature of the site
N_{ot}^{pv}	Temperature of PV cell in normal operation
v^{wt}	Wind speed [m/s]
v_0^{wt}	Location parameter of WT [m/s]
λ^{wt}	Shape factor of WT
c^{wt}	Scale parameter of WT
μ^{wt}	Average value of wind velocity
σ^{wt}	Standard deviation of wind velocity
P_{rated}^{wt}	Rated power of WT [kW]
$\alpha_1^{wt} - \alpha_3^{wt}$	Generation coefficients of WT
v_r^{wt}	Rated wind speed [m/s]
v_{ci}^{wt}/v_{co}^{wt}	Cut-in/Cut-out wind speed [m/s]
$P_g^{mt,min}$	Minimum power generation limits of MT gth [kW]
$P_g^{mt,max}$	Maximum power generation limits of MT gth [kW]
$P_g^{mt,ru}$	Ramp-up limits of MT gth [kW]
$P_g^{mt,rd}$	Ramp-down limits of MT gth [kW]
$\alpha_{1,g}^{mt} - \alpha_{3,g}^{mt}$	Cost function coefficient of MT gth
E^{fc}	FC potential obtained in an open circuit
F	Constant of Faraday
ε	Maximum allowed voltage deviation [%]
ΔG	Change in the free Gibbs energy
ΔS	Change of the entropy
R	Universal constant of the gases
P_{H_2}	Partial pressure of hydrogen
P_{O_2}	Partial pressure of oxygen
T^{fc}	FC operation temperature
T_r^{fc}	FC reference temperature
$\lambda_1^{fc} - \lambda_4^{fc}$	Parametric coefficient for the FC model
λ_5^{fc}	Parametric coefficient that relies on the FC and its operation state
R_m^{fc}	Internal resistance of FC [Ω]
R_c^{fc}	Constant resistance to the transfer of protons through the membrane [Ω]
$\alpha_{1,c}^{fc} - \alpha_{2,c}^{fc}$	Cost function coefficient of the cth FC
$P_b^{pev,tot}$	Capacity of the bth PEV battery [kW]
η^{pev+}/η^{pev-}	Charging/Discharging efficiencies of PEVs [%]
$\underline{SOC}^{pev}/\overline{SOC}^{pev}$	Minimum/Maximum SoC of the PEV battery [%]
SOC_{dep}^{pev}	Desired SoC of PEVs during the departure period [%]
$\alpha^{pev+}/\alpha^{pev-}$	Charging/Discharging costs of PEVs [$/kWh]

Decision variables

$P_{l+1,h}^{flow}$	Active power flow from bus lth at hour h [kW]
$Q_{l+1,h}^{flow}$	Reactive power flow from bus lth at hour h [kW]
$V_{l,h}$	Voltage magnitude at bus lth at hour h [V]
$P_{e,h}^{pv}$	Output power of PV eth at time h [kW]
PDF^{wt}	Weibull PDF of wind speed
$P_{e,h}^{wt}$	Power output of WT eth at hour h [kW]
$P_{g,h}^{mt}$	Power generation of MT gth at time h [kW]
$\sigma_{g,h}^{mt,uc}$	Commitment state of MT gth at time h [0,1]
$Cost^{mt}$	Operating cost of MT [$]
$Cost^{fc}$	Operating cost of FC [$]
$P_{c,h}^{fc}$	Power output of cth FC at hour h [kW]
$SOC_{b,h}^{pev}$	SoC of the bth PEV's battery at time h [%]
$P_{b,h}^{pev+}/P_{b,h}^{pev-}$	Charging/Discharging power of bth PEV at time h [kW]
$Cost_{b,h}^{pev}$	Operating cost of PEV bth at time h [%]

1.2. Literature review

Many researches have been carried out on energy management in charging and discharging of PEVs. Authors in [12] presented a charging strategy for PEVs in a microgrid, focusing on maximizing the use of distributed energy resources (DERs) to minimize the network's reliance on the upstream electricity grid. Nevertheless, this study only considered a single objective function of reducing the upstream energy demand by high PEV penetration. Using a modelled off-grid charging station for PEVs and hydrogen vehicles, [13] applied a mixed-integer linear programming (MILP) to compute the ideal ratings for an islanded photovoltaic (PV) and diesel generating station. The result showed

a 15% savings in operating cost of the diesel generator. Similarly, authors in [14] implemented a system with a PV, a battery, and a diesel hybrid system, using a heuristic technique to determine the ideal power system size for a PEV. Also, the total cost of the system declined by 5.21%. However, the amount of reduction seems insignificant when considering a large-scale deployment. Furthermore, in order to understand the impacts of the charging/discharging of PEVs on electricity consumption, the network reliance and stability, [15] developed a framework to analyse the effects of different grid-to-vehicle (G2V) and vehicle-to-grid (V2G) power levels on system stability. The results showed an increase in power demand during the afternoon period (i.e. when PEVs are charged) and a decline in demand during the morning period (i.e. when PEV owners are at work and PEVs are operating in V2G mode). However, the financial and safety implications were not examined. Conversely, [16] explored the financial impacts of slow and fast charging of PEVs while considering the drivers' behaviours. This research aimed to reduce annual investment expenses, lower power losses, and increase annual traffic flow. Regardless, a multi-objective (MO) evolutionary algorithm was deployed. Authors in [17] offered an orderly charging strategy for PEVs in a cloud–edge collaborative environment using deep learning. This approach used a central controller in the power grid at the cloud environment to develop a power supply strategy for all the charging stations. Also, the system predicted loads in residential areas, charging requirements, and output of RESs on the edge computing servers. Compared to the uncoordinated charging/discharging method, this procedure reduced the peak load to an off-peak difference and the standard deviation to around 30.13% and 16.94%, respectively. Using three case studies of home microgrid, DN, and utility function in a home grid, [18] implemented an MO techno-economic environmental optimization model in charging/discharging of PEVs. This method reduced the energy costs, the PEV's battery deterioration, CO_2 emissions, and power utilization by 88.2%, 67%, 34% and 90%, respectively. However, a more concise objective of CO_2 and operating cost reduction was presented in [19]. The authors used a more efficient technique to execute a power flow of a network with PVs, wind turbines (WTs), and PEVs. Also, the Monte Carlo simulation and the MO genetic algorithm were employed to handle the uncertainties of RESs and PEVs. Nonetheless, this central management technique has a high computational cost.

Authors in [20] developed a two-level energy management strategy considering flexible demand, storage devices and PEVs. Also, a stochastic-interval model is presented to handle the uncertainties of loads, RES, PEVs' behaviour, and energy pricing. A single-objective stochastic optimization framework is proposed in [21] for the optimal scheduling of a microgrid with RESs and PEVs to minimize the total operating cost using modified harmony search algorithm. The uncertainties of the RESs and the behaviour of the PEV owners in charging/discharging periods is taken into account. Furthermore, a techno-economic multi-level optimization strategy and a time varying price model is proposed in [22] to minimize the energy cost of a home microgrid and analyse the impact it has on voltage stability and reliability of the network. The proposed strategy develops an algorithm for smart charging/discharging of battery ESSs and PEVs to enhance energy efficiency. In [23], a multi-objective techno-economic scheduling of a smart distribution system is presented taking into account the diverse resources such as RESs, MT, and battery ESS. Besides, provision of both real and reactive power from battery ESS is considered in the scheduling of distribution system. Authors in [24] assessed the optimal allocation of integrated resources planning for sustainable energy-based hybrid microgrids considering PV, WT, and bio-energy resources. Besides, combined storage-based virtual-inertia support and PEV charging station-based demand-response support units for supply the required power and provide demand-side management, respectively. An optimal energy management strategy is proposed in [25] for a combined hydrogen, heat, and power microgrid with hydrogen fuelling stations for hydrogen vehicles (HVs), PEV parking lots and FC micro-CHP units to meet power and heat requirements. In order to enhance flexibility and investigate a low carbon microgrid, heat and power demand response programs are taken into consideration under the uncertainties of RESs in a MO information gap decision theory (IGDT) framework. However, the environmental factors is not considered as the objective function in [20–25]. An environmentally sustainable framework for optimal charging/discharging of PEVs in a smart microgrid was presented by [26]. It aimed to minimize the system's operating costs and reduce CO_2 emissions for different types of PEVs. Also, drivers' behaviours, driving patterns, and V2G functionality were investigated. The authors used a MO scheduling scheme in the charging/discharging of PEVs with an augmented e-constraint algorithm in reducing overall operating costs and CO_2 emissions. Authors in [27] allocated PEVs' charging stations and smart PV inverters simultaneously in DNs to optimize three objective functions, including power loss, voltage deviation, and voltage unbalance factor in a MO framework using a hybrid fuzzy Pareto dominance concept. Also, the scenario-based analysis is applied to model the uncertainties of the loads, PVs' power output, and the demand of PEV charging stations. Authors in [28] provided a multi-objective household-scale hybrid renewable energy system considering technical modelling of typical components such as PV, WT, battery. Besides, power can be supplied via the grid in grid-connected mode or can be generated by a MT in off-grid scenarios. However, the integration of fuel cells (FCs) and low-cost micro-turbines (MTs) are not considered in [26–28].

1.3. Contribution

Based on the literature reviewed, there is no work that concurrently integrates PV, WT, MT, and FC technologies with the DN aimed at minimizing the operating cost and CO_2 emissions in a stochastic framework. Table 1 gives a summary of this research and the reviewed literature. Accordingly, this paper aims to apply a MO stochastic optimization method under the uncertainties of renewable units, load consumption, and charging/discharging timing of PEVs. In particular, the Latin Hypercube Sampling (LHS) strategy is employed to control the mentioned uncertainties. It also focuses on incorporating DERs considering techno-economical and environmental factors to lower operating costs and CO_2 emissions simultaneously. The MO heuristic-based Firefly Algorithm (FA) is comprehensively applied in evaluating the energy management of PEVs with G2V and V2G technologies to minimize operating costs and CO_2 emissions in the DNs. The major research contributions (RCs) of this paper are summarized as follows to highlight the novelties:

RC1: Proposing a stochastic optimization framework applying MO heuristic-based FA to minimize the operating costs, lower CO_2 emissions, and improve the voltage profile of DNs as the result, simultaneously.

RC2: Investigating diverse environmental-friendly DERs including PV, WT, FC, MT to minimize PEVs charging reliance on the main grid and improve the voltage profile under the uncertainties of RESs, load demand, and arrival/departure period of PEVs.

RC3: Proposing a suitable charging method for PEVs considering driving patterns in an intelligent system to examine the role of the number of PEVs and their parking time in charging points (CPs) of PEVs.

1.4. Paper organization

The rest of the paper is laid out as follows. In Section 2, the model of Uncertainty and the proposed Mo FA are presented. In Section 3, the problem formulations is presented. Furthermore, the corresponding results of simulation are presented in Section 4. Finally, the paper is concluded with some points in Section 5.

Table 1
A comparative summary of this study and previous works.

Ref	Objective function	Heuristic approach	DER technology
[12]	• Minimize energy exchanged • Maximize RES integration	Probabilistic power flow algorithm and fmincon solver	PV/WT/Battery ESS/MT/PEV
[13]	• Operating cost minimization	–	PV/PEV
[14]	• Operating cost minimization	–	PV/Battery ESS/Diesel/PEV
[15]	• System reliability • System stability	Heuristic algorithm	Grid/PEV
[16]	• Minimize investment and operating costs • Maximize traffic flow	–	Grid/PEV
[17]	• Operating cost minimization	–	PV/WT/Grid/PEV
[18]	• Energy cost minimization • CO_2 minimization • Battery degradation minimization • Grid net exchange minimization	–	PV/Battery ESS/PEV
[19]	• Minimize operating cost • Power losses	Convolutional neural network and deep belief network	PV/WT/PEV
[20]	• Energy exchanging among prosumers • Collective assets	–	PV/Grid/Battery ESS/PEV
[21]	• Minimize operating cost	Modified harmony search algorithm	PV/WT/MT/FC/Battery ESS/PEV
[22]	• Minimize operating cost	–	PV/WT/CHP/Battery ESS/PEV
[23]	• Minimizing operation cost • Minimizing energy loss	–	PV/WT/Battery ESS/Diesel
[24]	• Minimize planning cost	–	PV/WT/Bio-Energy/MT/PEV
[25]	• Uncertainties of WTs and PVs	MO IGDT-Based robust approach	Grid/PV/WT/CHP/FC/HV/PEV
[26]	• Minimize procurement cost • CO_2 emission	Grey Wolf algorithm and weighed sum	PV/WT/CHP/PEV
[27]	• Power loss • Voltage deviation • Voltage unbalance factor	Hybrid fuzzy Pareto dominance	PV/PEV
[28]	• Minimizing net present cost • Minimizing total product environmental footprint	Genetic algorithm	PV/WT/Battery ESS/MT
This Study	• Minimize operating costs • CO_2 emissions	MO stochastic heuristic-based FA	PV/WT/FC/MT/PEV

2. Model description

The proposed system under study has renewable (non-dispatchable) resources including WT and PV, MT as a dispatchable resource, stationary and mobile ESSs including FC and PEVs in the radial distribution network. The mathematical formulation for implementing the proposed optimization framework is presented in the following sections.

2.1. Assumptions

The optimization problem is performed in this paper based on the following assumptions to improve the computation of the scheduling process:

1. To better investigate the practical calculations in real-world, the radial DN constraints are thoroughly proposed in this work so that the distribution power flow and its corresponding data of the impedance of the lines can properly calculate the power loss of the system.
2. Since the majority of the PEVs in the system are cars, the charging capacity of the PEV batteries of the big vehicles such as buses and trucks are not taken into account in this study. However, it can be noted that the generality of the model will not be lost by taking into consideration the big vehicles.
3. Due to the variable nature of renewable resources' output, load consumption, and commuting hours (charging and discharging hours of PEVs), it is assumed that the corresponding data in fluctuated between ± 10% of the determined values to better investigate the uncertainty of the parameters.

2.2. Model of uncertainty

In this paper, multiple scenarios of renewable generation, load consumption, and arrival/departure timing of PEVs are generated presenting the LHS strategy to determine the forecasting errors in a 24-h scheduling interval. The LHS strategy can be developed to the bi-stage method including the sampling stage and combination stage. In this study, 1000 samples were generated to consider the probabilistic characteristic of the uncertain parameters in the sampling stage. Therefore, the Cumulative Distribution Function (CDF) of the uncertain parameters is divided into 1000 segments with an equivalent probability of 1/1000 and converted to the Probability Distribution Function (PDF) to uniformly investigate the uncertain parameters. Accordingly, the following method can be proposed for each generated scenario-based variable, as demonstrated in Fig. 1 [29].

For k = 1 to 1000:

Step 1: An amount of probability is randomly appointed from each segment. The illustrative probability of the CDF at segment kth can be calculated based on Eq. (1).

$$prob_k = \frac{1}{1000}\left(rnd_u + k - 1\right) \tag{1}$$

where, $\mathrm{rnd}_u \in (0,1)$ represents a regularly distributed random weight.

Step 2: Eq. (2) indicates that the illustrative amount of probability is constantly adjusted into ρ_k using the reversed distribution function F^{-1}:

$$\rho_k = F^{-1}\left(prob_k\right) \tag{2}$$

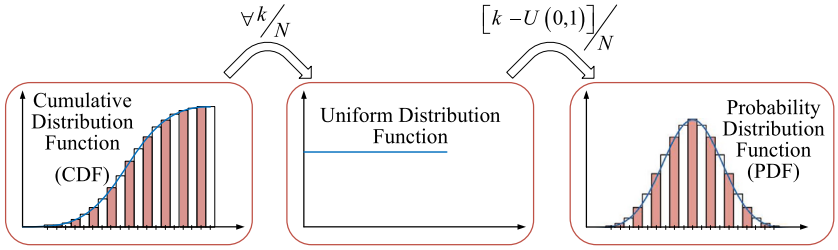

Fig. 1. Uncertainty modelling using Latin Hypercube sampling.

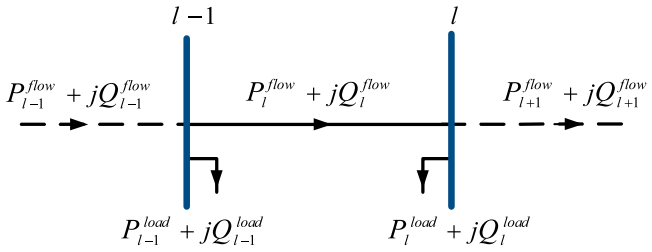

Fig. 2. Radial model of DN.

End For

Furthermore, to ensure the minimum correlation coefficients within the decision-making variables, the Cholesky factorization method is applied to merge the sampled amounts of the uncertain parameters. Also, a backward scenario reduction method is applied in the stochastic approach to decrease the number of generated scenarios and improve the calculation speed [30].

2.3. Firefly algorithm for optimization problem

FA was invented in 2010 to solve optimization problems supporting metaheuristic algorithms and is based on the flashing behaviour of fireflies. In addition, the firefly moves due to the light's intensity, and this behaviour is deployed in solving a global optimization issue [31]. As a result of its automatic subdivision and ability to deal with multi-modality, the FA outperforms other metaheuristic algorithms. Three basic rules are adopted for this algorithm as follows [32].

1. Although fireflies are unisex, they are constantly drawn to other fireflies regardless of sex.
2. If one firefly is brighter than the other, the flashing firefly is attracted to the brighter one. However, when both fireflies are of the same brightness, one will move chaotically. Also, the level of attractiveness varies with the amount of light.
3. The objective function determines the firefly's brightness.

The variation of attractiveness β with the distance r is expressed by Eq. (3).

$$\beta = \beta_0 e^{-\gamma r^2} \tag{3}$$

where the attractiveness at $r = 0$ is determined by β_0. The movement of firefly i to another brighter one j is described by Eq. (4).

$$x_i^{t+1} = x_i^t + \beta_0 e^{-\gamma r_{i,j}^2}(x_j^t - x_i^t) + \alpha_t \epsilon_i^t \tag{4}$$

where x_i is the position of a firefly in the iteration t, $\beta_0 e^{-\gamma r_{i,j}^2}(x_j^t - x_i^t)$ represents the attraction between firefly i and firefly j, ϵ_i^t is a vector of random numbers with a randomization parameter defined by α_t. This parameter is the initial randomness scaling factor and can be described as a randomly generated vector of either a uniform or Gaussian distribution. However, the firefly location could be adjusted sequentially by comparing and updating each pair in every iteration cycle.

The MO optimization could involve incorporating multiple objectives into a single objective, allowing the application of only one objective optimization algorithm with slight modification [33]. Accordingly, the FA is one of the suitable strategies that can be directly employed to handle MO problems as investigated by [34]. By extending the notions of the FA, the MO heuristic-based FA is developed, and its pseudo-code is presented in Algorithm 1. Another way to apply the FA in the optimization problem is to generate Pareto optimum fronts directly by expanding the FA approach. However, the objective functions and nonlinear constraints should be appropriately specified to achieve this. It begins by creating a population containing n fireflies scattered uniformly over the search space. This is accomplished by using uniformly distributed sampling methods. When the tolerance or a specified number of iterations is described, the iterations assess the fireflies' brightness and objective attributes, and evaluates each group of fireflies. Then, a randomized weight vector is created (with the total corresponding to 1) to create the combined best possible solution $g_\star^t$. The non-dominated solutions move to the following iteration. In theory, n non-dominated results locations could be found after several repetitions to approach the genuine Pareto optimum front. We could use the weighted sum to discover the best and most reliable $g_\star^t$ that minimizes a consolidated objective to execute randomized walks more effectively. The formulation of the uniformly distributed sampling method is presented in Eqs. (5)–(7).

$$\phi(x) = \sum_{n=1}^{N} w_n f_n \tag{5}$$

$$\sum_{n=1}^{N} w_n = 1 \tag{6}$$

$$w_n = \frac{\Pi_n}{n} \tag{7}$$

where Π_n are the numbers picked at random from a uniformly distributed sampling method. To be certain that $\sum \Pi_n = 1$ after creating N evenly distributed values, a re-scaling procedure is conducted. Also, it is important to note that w_n must be selected at random through every iteration, as a result of which the non-dominated option can analyse in a variety of ways with Pareto front. A firefly travels if it is not influenced by other fireflies in the context of the Pareto front. Accordingly, Eq. (4) can be rewritten as Eq. (8).

$$x_i^{t+1} = g_\star^t + \alpha_t \epsilon_i^t \tag{8}$$

where $g_\star^t$ represents the ultimate option for a given collection of random weights that has been found thus far. Moreover, because of the iterations progress, the randomness could be decreased similarly to how metaheuristics and other random reduction approaches work. Furthermore, the initial randomness scaling factor, α_t, is defined based on the Eq. (9).

$$\alpha_t = \alpha_0 \delta^t \tag{9}$$

where α_0 represents the randomization factor at the initial stage. Besides, δ has a value between 0 and 1 and is set to be 0.9 in this paper.

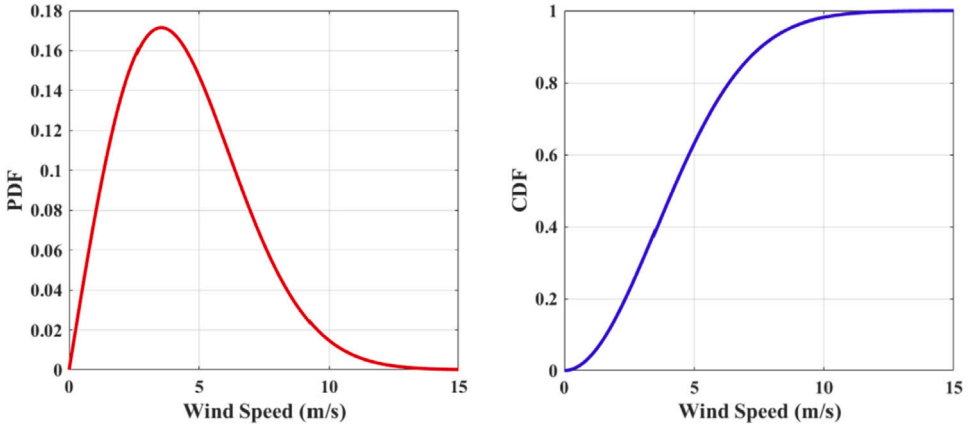

Fig. 3. Weibull's PDF and CDF for wind speed.

Algorithm 1 The Pseudo-code of MO heuristic-based FA.

Define objective functions $f_1(X), \cdots, f_n(x)$ where $x = (x_1, \cdots, x_d)^\tau$;
Initialize a population of n fireflies $x_i (i = 1, 2, 3, n)$;
while t> Max generation **do**
  for $i,j = 1{:}n$ (all n fireflies) **do**
    Evaluate the approximations to the Pareto fronts j and i for $i \neq j$.
    if Pareto front j dominates Pareto front i **then**
      Move firefly i towards j using $x_i^{t+1} = x_i^t + \beta_0 \exp^{-\gamma r_{i,j}^2}(x_j^t - x_i^t) + \alpha_t \epsilon_i^t$
      Generate new ones if the moves do not satisfy all the constraints
    end if
    if no non-dominated solutions can be found **then**
      Generate random weights $w_n(1, \cdots, n)$
      Find the best solution $g_\star^t$ to minimize ϕ in $\phi(x) = \sum_{n=1}^{N} w_n f_n$
      Random walk around $g_\star^t$ using $x_i^{t+1} = g_\star^t + \alpha_t \epsilon_i^t$
    end if
    Update and pass the non-dominated solutions to next iterations
  end for
  Sort and find the current best approximation to the Pareto front
  Update $t \longleftarrow t + 1$
end while

3. Problem formulations

The formulation of the proposed FA optimization problem is described in the following sections.

3.1. Distribution power flow

Fig. 2 illustrates a radial model of DN. The distribution power flow equations associated with bus lth of the DN are demonstrated in Eqs. (10)–(13) [35]. In this model, the impedance of the lines are represented as $r_l + jx_l$.

$$P_{l+1,h}^{flow} = P_{l,h}^{flow} - r_l \frac{\left(P_{l,h}^{flow}\right)^2 + \left(Q_{l,h}^{flow}\right)^2}{\left(V_{l,h}\right)^2} - P_{l+1,h}^{load} \tag{10}$$

$$Q_{l+1,h}^{flow} = Q_{l,h}^{flow} - x_l \frac{\left(P_{l,h}^{flow}\right)^2 + \left(Q_{l,h}^{flow}\right)^2}{\left(V_{l,h}\right)^2} - Q_{l+1,h}^{load} \tag{11}$$

$$\left(V_{l+1,h}\right)^2 = \left(V_{l,h}\right)^2 - 2\left(r_l.P_{l,h}^{flow} + x_l.Q_{l,h}^{flow}\right) + \left[\left(r_l\right)^2 + \left(x_l\right)^2\right] \frac{\left(P_{l,h}^{flow}\right)^2 + \left(Q_{l,h}^{flow}\right)^2}{\left(V_{l,h}\right)^2} \tag{12}$$

$$1 - \varepsilon \leq V_{l,h} \leq 1 + \varepsilon \tag{13}$$

3.2. Modelling of PV cell

The generated power from PV arrays is fed into an inverter, converting it from direct current to alternating current at an appropriate voltage level before being connected to the power grid. PV cells harness solar energy, which is a renewable energy source. Hence, they are eco-friendly, require minimal maintenance and have a high potential to lower electricity bills. However, the power generated by PV cells varies greatly, with solar angle and intensity being the two most influencing factors. The PV's output power is computed using Eq. (14) [36]. Also, the uncertainties in PV generation are modelled using the PDF.

$$P_{e,h}^{pv} = P_{stc}^{pv}.G^{pv}/G_{stc}^{pv}.\left[1 + \lambda_{mpt}^{pv}(T_c^{pv} - T_{ref}^{pv})\right] \tag{14}$$

The T_c^{pv} is obtained from Eq. (15).

$$T_c^{pv} = T_a^{pv} + \frac{(N_{ot}^{pv} - 20)}{0.8}.G^{pv} \tag{15}$$

3.3. Modelling of WT

WT blades capture kinetic energy when they spin. The kinetic energy is converted to mechanical energy, which drives a generator to produce electricity. The electricity from a WT is renewable, cost-effective and environmentally friendly. However, the power from a WT is intermittent and highly reliant on wind speed and the mechanical characteristics. Therefore, the uncertainties in wind speed are simulated using the Weibull PDF. Fig. 3 illustrates the proposed wind speed's CDF and Weibull PDF. Eqs. (16)–(18) show the formulation of the PDF for WTs [37].

$$\mathrm{PDF}^{wt}(v) = \frac{\lambda^{wt}}{c^{wt}}\left[\frac{v^{wt} - v_0^{wt}}{c^{wt}}\right]^{\lambda^{wt}-1}.\exp\left(-\left[\frac{v^{wt} - v_0^{wt}}{c^{wt}}\right]^{\lambda^{wt}}\right) \tag{16}$$

$$\lambda^{wt} = \left(\frac{\sigma_v^{wt}}{\mu_v^{wt}}\right)^{-1.086} \tag{17}$$

$$c^{wt} = \frac{\mu_v^{wt}}{T^{wt}(1 + 1/\lambda^{wt})} \tag{18}$$

The power output of WT, P_t^{wt}, is a function of the wind speed which is formulated by Eq. (19) [38].

$$P_{e,h}^{wt} = \begin{cases} 0 & 0 < v^{wt} < v_{ci}^{wt} \\ P_{rated}^{wt}.\left(\alpha_1^{wt} + \alpha_2^{wt} v + \alpha_3^{wt} v^2\right) & v_{ci}^{wt} < v^{wt} < v_r^{wt} \\ P_{rated}^{wt} & v_r^{wt} < v^{wt} < v_{co}^{wt} \end{cases} \tag{19}$$

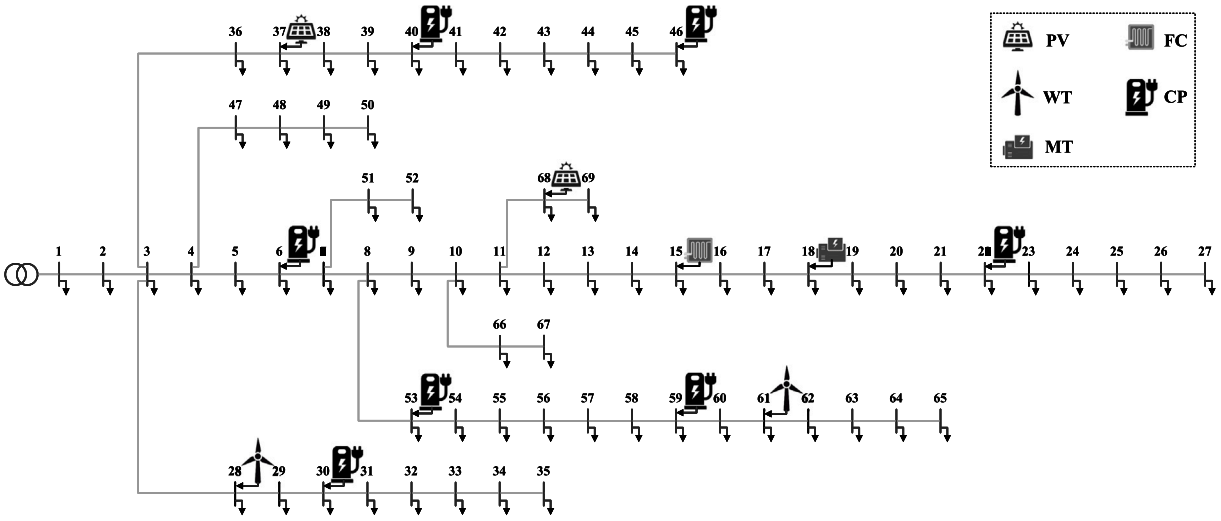

Fig. 4. The modified IEEE Bus 69 radial network.

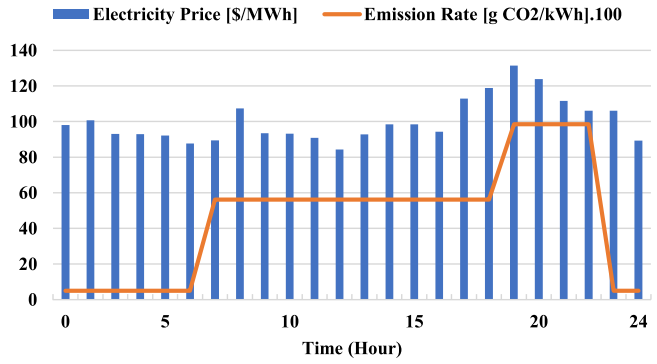

Fig. 5. Hourly electricity price and emission rate.

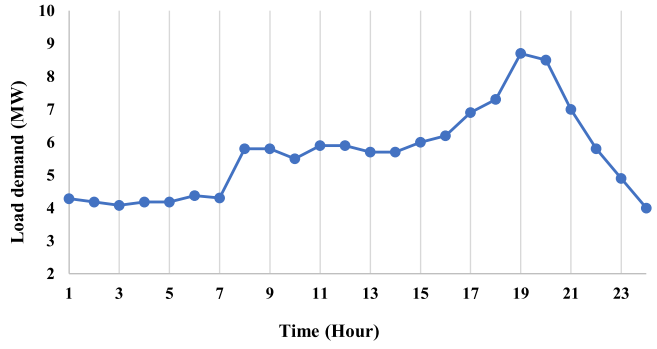

Fig. 6. Hourly forecasted load profile.

The generation coefficients of WT are obtained by Eqs. (20)–(22).

$$\alpha_1^{wt} = \frac{v_{ci}^{wt}}{(v_{ci}^{wt} - v_r^{wt})^2}\left[v_{ci}^{wt} + v_r^{wt}\right] - 4\left[v_{ci}^{wt} v_r^{wt}\right]\left(\frac{v_{ci}^{wt} - v_r^{wt}}{2v_r^{wt}}\right)^3 \tag{20}$$

$$\alpha_2^{wt} = \frac{1}{(v_{ci}^{wt} - v_r^{wt})^2}\left[4(v_{ci}^{wt} + v_r^{wt})\left(\frac{v_{ci}^{wt} + v_r^{wt}}{2v_r^{wt}}\right)^3\right] - (3v_{ci}^{wt} + v_r) \tag{21}$$

$$\alpha_3^{wt} = \frac{1}{(v_{ci}^{wt} - v_r^{wt})^2}\left[2 - 4\left(\frac{4v_{ci}^{wt} + v_r}{2v_r^{wt}}\right)^3\right] \tag{22}$$

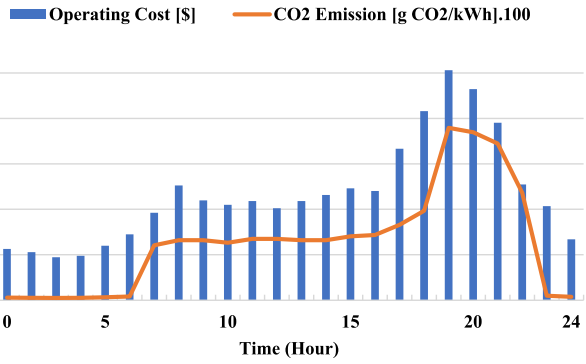

Fig. 7. The operating costs and CO_2 emissions per hour in the base system.

3.4. Modelling of MT

MT is one of the beneficial DER in an DN. MTs are dispatchable and have low investment costs, high reliability, and longer run-time. Eqs. (23)–(25) guarantee that the output of each MT be within its allowed generation limits. The commitment states, up/down ramp-rate boundaries, and start-up/shut-down states are considered in the MT generation constraints [39].

$$P_g^{mt,min}.\sigma_{g,h}^{mt,uc} \le P_{g,h}^{mt} \le P_g^{mt,max}.\sigma_{g,h}^{mt,uc} \tag{23}$$

$$P_{g,h-1}^{mt} - P_{g,h}^{mt} = P_g^{mt,ru} \tag{24}$$

$$P_{g,h}^{mt} - P_{g,h-1}^{mt} = P_g^{mt,rd} \tag{25}$$

The generation cost of MT can be expressed by a polynomial quadratic formulation as shown in Eq. (26).

$$Cost_{g,h}^{mt} = \alpha_{1,g}^{mt} + \alpha_{2,g}^{mt} P_{g,h}^{mt} + \alpha_{3,g}^{mt} (P_{g,h}^{mt})^2 \tag{26}$$

3.5. Modelling of FC

FCs are electrochemical energy conversion systems that use hydrogen or other fuels to generate electricity and produce water as a by-product. FCs can deliver high-efficiency electrical power with low operational noise and hardly any environmental pollutants. Also, FCs come in diverse forms, each with its chemical properties. Therefore,

Table 2
MT generation cost parameters and rate of CO_2 emission.

α_1^{mt} ($)	α_2^{mt} ($/kWh)	α_3^{mt} ($/kWh^2)	$\theta_h^{CO_2,mt}$ (kg/kWh)	$P^{mt,min}$ (kW)	$P^{mt,max}$ (kW)
10	0.0133	0.002	0.890	50	1000

Table 3
FC generation cost parameters and rate of CO_2 emission.

α_1^{fc} ($)	α_2^{fc} ($/kWh)	α_3^{fc} ($/kWh^2)	$\theta_h^{CO_2,fc}$ (kg/kWh)	$P^{fc,min}$ (kW)	$P^{fc,max}$ (kW)
45	0.375	–	0.477	100	1000

Table 4
Parking time and location of PEV's CPs.

CPs	Number of PEVs	Parking time of PEVs	
		Home	Workplace
#1	200	1 AM–6 AM & 5 PM–12 AM	8 AM–3 PM
#2	200	1 AM–6 AM & 5 PM–7 PM	8 AM–3 PM
#3	100	1 AM–5 AM & 5 PM–12 AM	–
#4	200	1 AM–5 AM & 5 PM–7 PM	–
#5	150	1 AM–9 AM & 1 PM–6 PM & 10 PM–12 AM	–
#6	100	1 AM–6 AM	–
#7	50	1 AM–6 AM	8 AM–3 PM

Table 5
Characteristics of PEV battery.

Charging time	Discharging time	$P^{pev,tot}$	Max Mileage	Charging rate	Discharging rate
1 AM to 6 AM	6 PM to 12 AM	24 kWh	170 km	6 kW	6 kW

this paper employs the polymer electrolyte membrane type of FC in the system design. This type of FC consists of a current collector that includes a gas channel, a catalyst layer plus a gas diffusion layer on the cathode and anode area, and an ion conductive polymer membrane. FCs' merits include more prolonged running conditions, rapid refuelling compared with the time required for battery recharging, rapid start-up, protracted lifespan, good durability, efficiency, reduced wear and tear, high power density. The FC model consists of three interconnected subsystems: anode and cathode flow, stack voltage, and membrane hydration [40]. The current–voltage relationship is generally provided in the polarization curve model, which is the plot of FC voltage, V^{fc} versus current density, I^{fc}. The I^{fc} is determined as stack current per unit of cell active area, $I^{fc} = I_{st}^{fc}/A^{fc}$, given that FCs are serially connected in the stack form. The total stack voltage can be defined by multiplying the FC voltage, V^{fc}, by the number of established cells, n of the stack, as $V_{st}^{fc} = nV^{fc}$. Thus, the stack power of FCs is defined as Eq. (27) [41].

$$P_{st}^{fc} = V_{st}^{fc}.I_{st}^{fc} = (nV^{fc})(A^{fc}I^{fc}) \tag{27}$$

The FC voltage is determined by subtracting the FC losses or over-voltages from the FC open circuit voltage, E^{fc}, and is calculated based on Eqs. (28)–(32).

$$V^{fc} = E^{fc} - V_{act}^{fc} - V_{\Omega}^{fc} - V_{conc}^{fc} \tag{28}$$

where

$$E^{fc} = \frac{1}{2F}\left(\Delta G + \Delta S(T^{fc} - T_r^{fc}) + RT^{fc}\left[\ln(P_{H_2}) + \frac{1}{2}\ln(P_{O_2})\right]\right) \tag{29}$$

The activation over-potential, V_{act}^{fc} containing anode and cathode can be defined as Eq. (30).

$$V_{act}^{fc} = -\left[\lambda_1^{fc} + \lambda_2^{fc}.T^{fc} + \lambda_3^{fc}.T^{fc}.\ln\left(\frac{P_{O_2}}{(5.1).10^6 e^{\frac{-498}{T^{fc}}}}\right) + \lambda_4^{fc}.T^{fc}.\ln(I^{fc})\right] \tag{30}$$

The voltage drop caused by the mass transport, V_{conc}^{fc} can be defined as Eq. (31).

$$V_{conc}^{fc} = -\lambda_5^{fc}.\ln\left(1 - \frac{(I^{fc}/A^{fc})}{(I^{fc}/A^{fc})^{max}}\right) \tag{31}$$

The ohmic voltage drop, V_{Ω} is also defined in Eq. (32).

$$V_{\Omega} = I^{fc}\left(R_m^{fc} + R_c^{fc}\right) \tag{32}$$

Furthermore, the operation cost of FC can be defined by Eq. (33).

$$Cost_{c,h}^{fc} = \alpha_{1,c}^{fc} + \alpha_{2,c}^{fc}P_{c,h}^{fc} \tag{33}$$

3.6. Modelling of G2V and V2G for PEVs

Many factors affect PEV operation, including PEV battery power, arrival and departure periods, and the initial state of charge (SoC). The model of PEV is defined by Eqs. (34)–(38) [42]. Eq. (34) indicates the energy balance of PEV batteries.

$$SOC_{b,h}^{pev} = SOC_{b,h-1}^{pev} + \left(P_{b,h}^{pev+}.\eta^{pev-} - P_{b,h}^{pev-}/\eta^{pev-}\right)/P_b^{pev,tot} \tag{34}$$

At any given time, the SoC of PEV batteries must be in its allowed capacity as indicated in Eq. (35).

$$\underline{SOC}^{pev} \le \mathrm{SOC}_{b,h}^{pev} \le \overline{SOC}^{pev} \tag{35}$$

Eqs. (36) and (37) indicate the upper/lower limits of charging/discharging of PEV battery.

$$0 \le P_{b,h}^{pev+} \le P_b^{pev,tot}.\left(1 - SOC_{b,h-1}^{pev}\right)/\eta^{pev+} \tag{36}$$

$$0 \le P_{b,h}^{pev-} \le P_b^{pev,tot}.SOC_{b,h-1}^{pev}.\eta^{pev-} \tag{37}$$

Furthermore, each PEV should be charged to its desired SoC during the departure period as shown in Eq. (38).

$$SOC_{b,h^{dep}}^{pev} = SOC_{dep}^{pev} \tag{38}$$

The cost of charging/discharging the PEVs can be calculated by Eq. (39).

$$Cost_{b,h}^{pev} = (\alpha^{pev+}P_{b,h}^{pev+}) + (\alpha^{pev-}P_{b,h}^{pev-}) \tag{39}$$

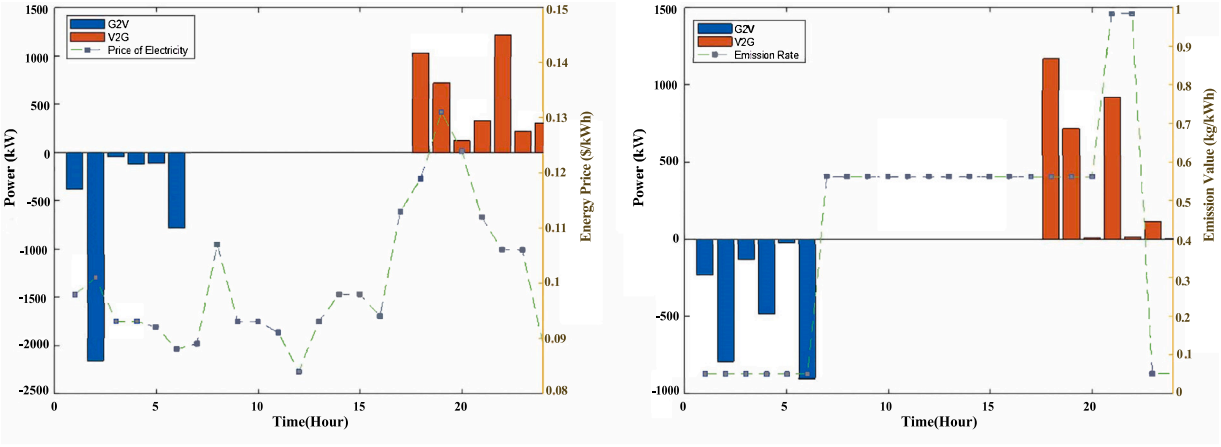

((a)) CS1 ((b)) CS2

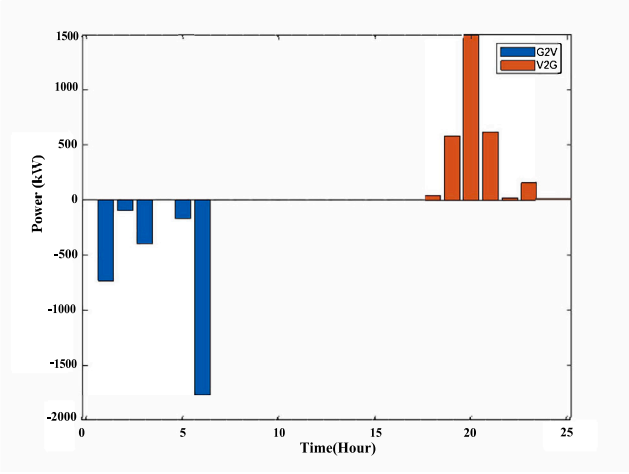

((c)) CS3

Fig. 8. Load and CO_2 profile of Electric Vehicles in G2V and V2G mode.

3.7. Power balance constraint

The power balance constraint at time h is represented by Eq. (40).

$$\sum_{g} P_{g,h}^{mt} + \sum_{c} P_{c,h}^{fc} + \sum_{e}(P_{e,h}^{pv} + P_{e,h}^{wt}) + \sum_{b}(P_{b,h}^{pev-} - P_{b,h}^{pev+}) + P_{h}^{gr} = \sum_{l} P_{l,h}^{load} + P_{h}^{loss} \tag{40}$$

where P_h^{gr} is the power purchased from the main grid and P_h^{loss} is the power loss at time h, which is calculated based on the proposed power flow equations.

3.8. Proposed objective functions

The proposed strategy focuses on minimizing a MO function including the total operating costs, $Cost^{dn}$, and CO_2 emissions, Em^{dn}, as expressed in Eq. (41).

$$F^{MO} = \text{Min } \{Cost^{dn}, Em^{dn}\} \tag{41}$$

The total operating cost can be calculated as given in Eq. (42) [43].

$$Cost^{dn} = \sum_{s}\rho_s \sum_{h}\Big[\sum_{g} Cost_{g,h,s}^{mt} + \sum_{c} Cost_{c,h,s}^{fc} + \sum_{b} Cost_{b,h,s}^{pev} + \sum_{e} Cost_{e,h,s}^{res} + Cost_{h,s}^{gr}\Big] \tag{42}$$

where ρ_s is the probability of scenario sth. $Cost_{e,h}^{res}$ represents the generation cost of RESs including WTs and PV cells at time h and $Cost_h^{gr}$ represents the cost of purchasing power from the main grid at time h. The generation cost of RESs is calculated by Eq. (43).

$$Cost_{e,h}^{res} = \sum_{e} \alpha_h^{res}(P_{e,h}^{pv} + P_{e,h}^{wt}) \tag{43}$$

where α_h^{res} is the cost coefficient of generating RESs at time h. Eq. (44) shows the cost of energy purchased from the main grid when there is a power deficiency.

$$Cost_h^{gr} = \alpha_h^{gr} P_h^{gr} \tag{44}$$

where α_h^{gr} is the coefficient cost of energy purchased from the main grid at time h. Furthermore, there are two parts in CO_2 emission reduction. The emissions of MT, FC, and the energy absorbed from the main DN are reduced. The CO_2 minimization function is shown in Eq. (45) [26,43].

$$Em^{dn} = \sum_{s}\rho_s \sum_{h}\left[Em_{h,s}^{dg} + Em_{h,s}^{gr}\right] \tag{45}$$

$$Em_h^{dg} = \theta_h^{CO_2,mt} \sum_{g} P_{g,h}^{mt} + \theta_h^{CO_2,fc} \sum_{c} P_{c,h}^{fc} \tag{46}$$

$$Em_h^{gr} = \theta_h^{CO_2,gr} P_h^{gr} \tag{47}$$

where Em_h^{dg} is the total emission produced by the MTs and FCs at time h (in kg CO_2) and $Em_{h,s}^{gr}$ is the emission generated energy purchased from the main grid at time h (in kg CO_2). Also, $\theta_h^{CO_2,mt}$, $\theta_h^{CO_2,fc}$, and $\theta_h^{CO_2,gr}$ represent the CO_2 emission rate of MT, FC and main grid, respectively (in kg CO_2/kWh).

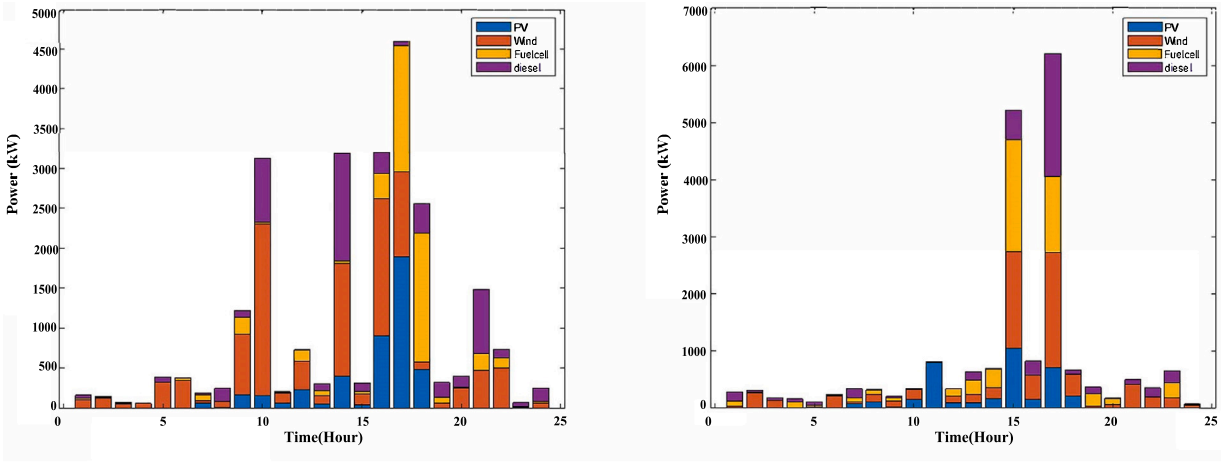

((a)) CS1

((b)) CS2

((c)) CS3

Fig. 9. Power generation of DERs.

4. Illustrative implementation

The proposed MO optimization method is applied on a modified IEEE bus 69 system radial DN as presented in Fig. 4. The remodelled radial network comprises two WTs located at Buses 28 and 61, two PV systems at Buses 37 and 68, one MT set at Bus 18, and one FC unit at Bus 15. The MT and FC data of generation cost and CO_2 emission are given in Tables 2 and 3, respectively. Table 4 illustrates the number of PEVs and their parking time at respective CPs [44]. In addition, the characteristics of PEV battery is indicated in Table 5. In this paper, the PEV's charging cycle begins at 01:00 and ends at 06:00, while the discharging cycle starts at 18:00 and continues till 00:00 h when electricity prices and demands are high. Fig. 5 shows the hourly electricity prices and CO_2 emission rate. Besides, Fig. 6 presents hourly forecasted load profile of DN.

The unmodified IEEE 69 bus system is considered as the base system for evaluating the performance of the recommended algorithm. The base system is tested without the inclusion of any DER. Accordingly, the power balance of load consumption and power purchased from main grid is proposed as the problem constraint. Under the base system, the operating cost is estimated at \$11 223.32 and the CO_2 emissions is estimated around 61 493.9 $kgCO_2$ as illustrated in Fig. 7.

Table 6 demonstrates the various simulation case studies (CSs). First, in CS1, only the minimization of the operating costs is considered. Then, in CS2, only the minimization of CO_2 emissions is considered.

Table 6
Case study definition.

Case study	Total operating cost	CO_2 emissions	MO FA
CS1	Yes	No	No
CS2	No	Yes	No
CS3	Yes	Yes	Yes

Finally, CS3 applies the FA to simultaneously reduce operating costs and CO_2 emissions as well as improve the voltage profile of DN.

Fig. 8 shows the V2G and G2V operations for the proposed CSs. Based on Figs. 8(a) and 8(b), the PEVs are charged between 1 AM and 6 AM, when the electricity's price is low and discharged at peak load hours of 6 PM to 12 AM, when the price of electricity is high. Compared to the base case, the CS1 reduces the operating cost by 50% with considering the uncertainties and by 46% without considering uncertainties. In lowering the CO_2 emissions in CS2, a flexible PEVs scheduling is recommended, such that PEVs operate in a G2V mode during low emission rates (between 1 AM and 6 AM) and in V2G mode at the time of high emission rates (from 6 PM to 12 AM). When the CO_2 emission in CS2 is compared with the based case, its value declined by 55% considering the uncertainties and by 54% without considering uncertainties. In employing the MO strategy in CS3, it is observed that the system is more cost-effective and environmentally beneficial to charge the PEVs between 1 AM and 6 AM and discharge them from 6 PM to 12 AM, as illustrated in Fig. 8(c). During the

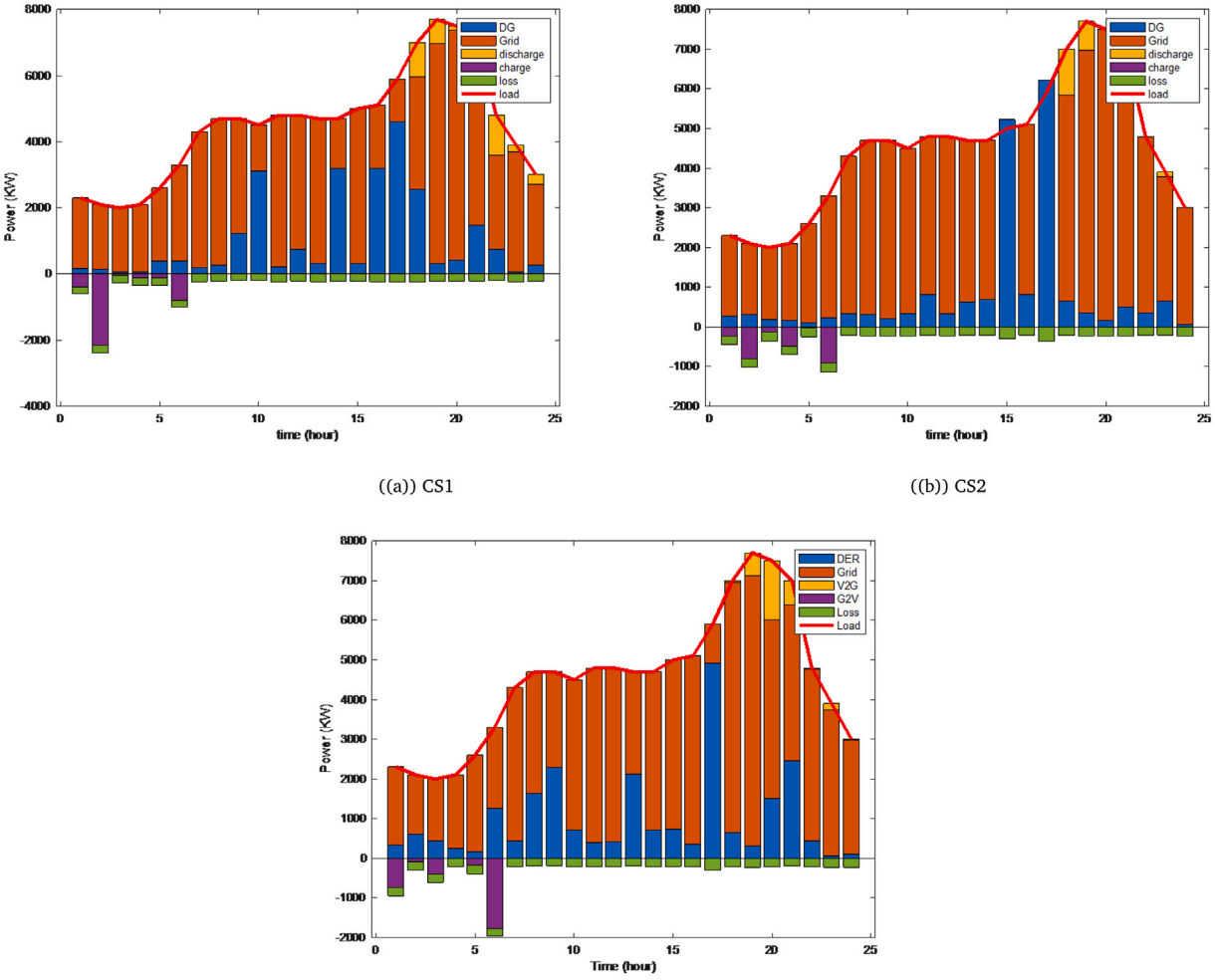

Fig. 10. Total power balance.

Table 7
Summary of operating costs, CO_2 emissions, and energy losses.

Case study	Daily operating cost [$]	Daily CO_2 emissions [kg]	Total energy loss [kW]
Base case	11 223.32	61 493.90	7799.39
CS1 (without uncertainty)	5960.98	–	5328.74
CS1 (with uncertainty)	5500.63	–	5161.98
CS2 (without uncertainty)	–	27 487.50	5578.44
CS2 (with uncertainty)	–	27 888.60	5900.48
CS3 (without uncertainty)	5791.10	27 553.70	5578.44
CS3 (with uncertainty)	5681.00	27 929.90	5900.48

recommended G2V operational period, the emission rate and electricity price are low, while both parameters are high during the V2G time mode. Using the proposed MO framework, the CO_2 emission reduced by 55% and 54% with and without considering uncertainties, respectively, compared to the based case. Conversely, the operating cost declined by 49% considering the uncertainties and by 48% without considering uncertainties.

Fig. 9 represents the power generated by DERs in the various CSs. It is clear from Fig. 9 that the power output of MT in CS3 is reduced markedly and FC power generation is enhanced significantly compared to CS1 and CS2. It can also be seen that considering the proposed MO structure, the employing of RESs has generally increased. Furthermore, Fig. 10 indicates the total power balance in the various CSs. It can be seen that on average, most of the energy for the low-emission operation is from the FC unit, which generates less CO_2 emissions than the MT. Similarly, PVs and WTs also contribute more power than MT for minimizing CO_2 emissions. Fig. 11 shows the CO_2 emission and energy losses in the CSs. It is clear that the energy losses are equal for all CSs, while the CO_2 emission in CS3 is slightly enhanced for both scenarios with and without considering the uncertainty compared to the CS2. Accordingly, the proposed MO strategy increases the CO_2 emission by 0.15% and 0.24% for scenarios with and without considering the uncertainty, respectively. Besides, by applying DERs and PEVs in the proposed algorithm, the voltage profile in CS3 is improved by 6%, as shown in Fig. 12, thus, enhancing the system's performance.

Finally, Table 7 provides a summary of the operating costs and CO_2 emissions in the CSs. It can be seen that the operating cost in CS3 is reduced for scenario without uncertainty while is enhanced for scenario with uncertainty compared to CS1. Also, the CO_2 emissions in CS3 are increased for both scenario without and with uncertainty compared

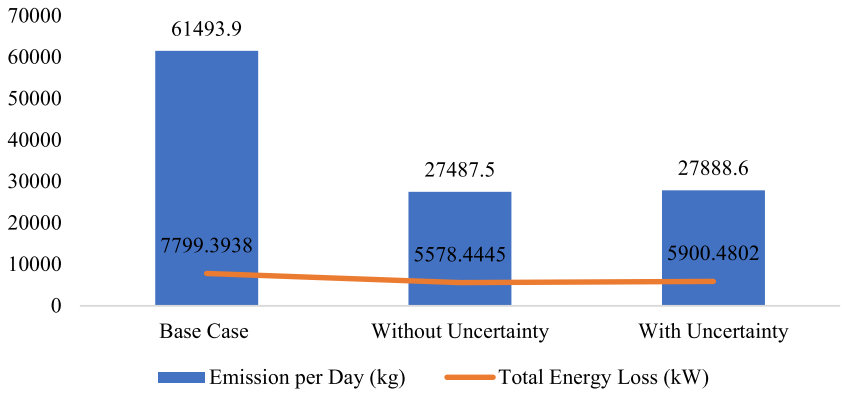

((a)) CS2

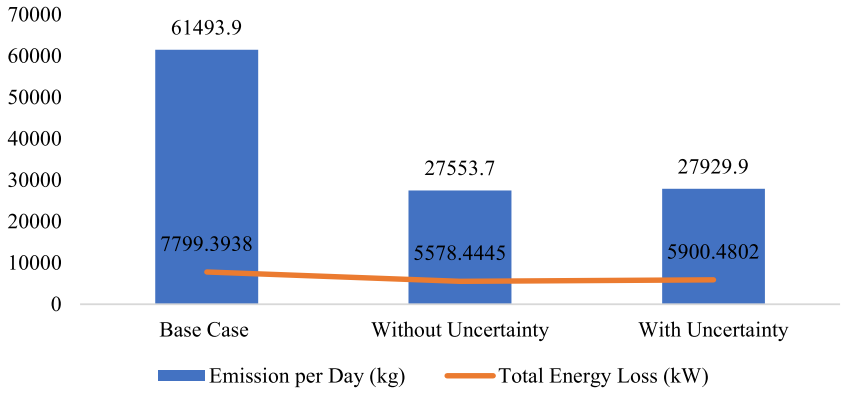

((b)) CS3

Fig. 11. CO_2 emission and energy losses.

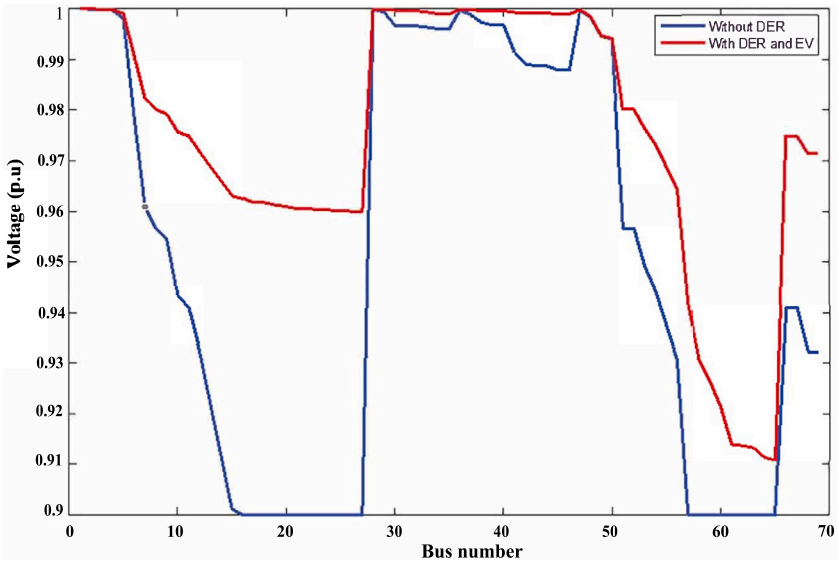

Fig. 12. Voltage profile of the modified IEEE 69 bus system in CS3.

to CS2. Therefore, it can be generally mentioned that investigating uncertainty in the optimization algorithm reduces operating costs and increases CO_2 emissions compared to the scenarios without uncertainty. Furthermore, Table 8 compares the CO_2 emission and financial benefits for PEVs owners in CS3 with and without PEVs. It is clear that the PEVs owners can save around $787 daily in costs and reduce 33 564 kg CO_2 with considering PEVs in the proposed algorithm.

For the sake of a detailed analysis, the proposed FA results are compared with Particle Swarm Optimization (PSO) algorithm for all CSs in Figs. 13–15. Fig. 13 demonstrates the linearized Pareto front for the proposed FA and the presented PSO results in CS3. As it is clear,

Table 8
CO_2 and financial benefits for PEVS owners in CS3.

Case study	Daily operating cost [$]	Daily CO_2 emissions [kg]	Revenue for PEVs owners [$]
Without V2G operation	11 223.32	61 493.9	0
With V2G operation	5681.00	27 929.9	787.724

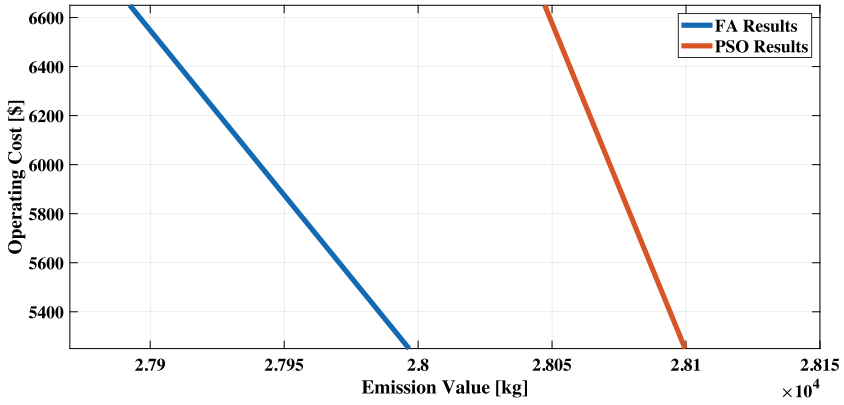

Fig. 13. Linearized Pareto front for FA and PSO results in CS3.

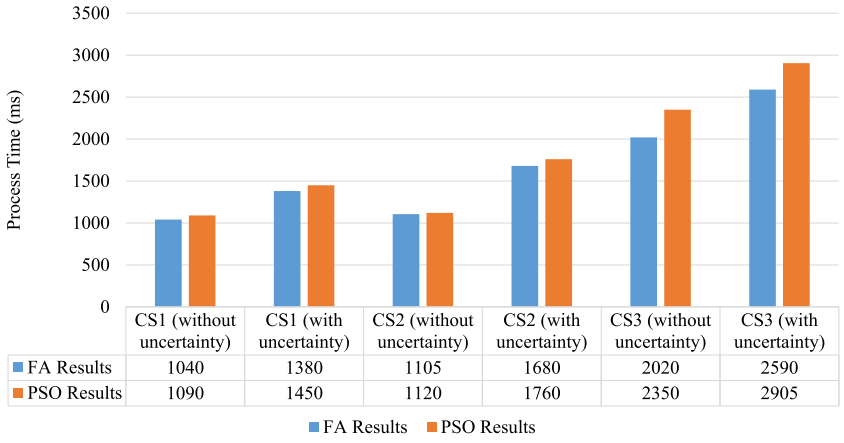

Fig. 14. Process time taken for FA and PSO on all CSs.

the FA performs much better compared to the PSO. As the point of applying either the FA or PSO is speed rather than extreme accuracy, the FA seems to perform comparably well to the PSO for the similar scale optimization problems. Furthermore, the process time taken for FA and PSO to obtain the final results on all CSs is illustrated in Fig. 14. It can be seen that these times are actually faster for FA, given that both algorithms were run on the same processor, but the results indicates that the FA runs a little faster compared to the PSO. Moreover, Fig. 15 shows the number of iterations to find the global minimum result for the proposed CSs. It is clear that the FA performs better compared to the PSO so that for proposed CSs, and particularly the single-objective ones, the FA is much more efficient than PSO.

5. Conclusion

This paper presents a flexible optimization approach for charging/discharging of PEVs by simultaneously reducing the operating cost and CO_2 emissions of the network applying a multi-objective heuristic-based Firefly Algorithm in a stochastic framework under the uncertainties of RESs, load consumption, and charging/discharging timing of PEVs. In addition, small-scale DERs including photovoltaic cells, wind turbines, fuel cell, and micro-turbine are presented to reinforce the network and facilitate the mass adoption of the PEVs. The proposed strategy is tested using a modified IEEE 69 bus system in MATLAB software and the simulation results demonstrate the effectiveness of the proposed multi-objective strategy. The main results can be highlighted as follows:

1. A 48% reduction operating costs and a 55% reduction in CO_2 emissions in the modified network are achieved with the proposed FA optimization framework.
2. The results recommend operating the PEVs in grid-to-vehicle mode at low-priced electricity and low CO_2 emission rate hours, and vehicle-to-grid operations when electricity price and CO_2 emissions rate are high.
3. The PEV owners financially benefit from the proposed system through their participation in the energy market through the vehicle-to-grid services by saving around $787.7 daily in operating costs.
4. The voltage profile of the network is improved up to 6%, thus, further enhancing the overall system's stability and reliability.
5. Finally, based on the presented comparison between the proposed FA and PSO, it can be noted that the proposed optimization framework in this paper is faster and the total iterations to achieve the best value is also lower compared to the PSO results.

Accordingly, the proposed heuristic-based Firefly Algorithm has proven effective in achieving an overall reduction in operating costs,

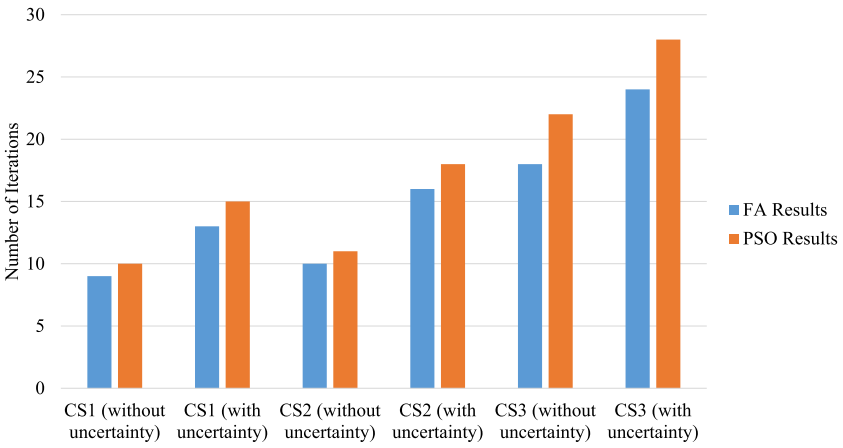

Fig. 15. Number of iterations to find the global minimum result of all CSs.

minimizing CO_2 emissions and improving network stability. According to the structure of the proposed optimization algorithm, the multi-energy career networks can be studied to investigate the flexibility of the multi-energy networks. In addition, the life cycle assessment can be also proposed in future researches to realize the environmental benefits of the PEVs in the proposed system.

CRediT authorship contribution statement

Seyed Ehsan Ahmadi: Methodology, Software, Investigation, Conceptualization, Formal analysis, Writing – original draft. **S. Mahdi Kazemi-Razi:** Investigation, Conceptualization, Formal analysis, Writing – original draft. **Mousa Marzband:** Supervision, Funding acquisition, Investigation, Conceptualization, Formal analysis, Writing – review & editing. **Augustine Ikpehai:** Validation, Investigation, Formal analysis, Writing – review & editing. **Abdullah Abusorrah:** Validation, Investigation, Formal analysis, Writing – review & editing.

Declaration of competing interest

The authors declare that they have no known competing financial interests or personal relationships that could have appeared to influence the work reported in this paper.

Data availability

The authors do not have permission to share data.

Acknowledgements

This work was supported from DTE Network+ funded by EPSRC grant reference EP/S032053/1, United Kingdom. The authors would like to thanks Mr. Alex S. Daramola and Mr. Nnamdi Anthony Iwoba for their assistance and contribution during data collection, simulation, and analysis the corresponding results.

References

[1] R. United Nations, Code red' for human driven global heating, warns UN chief. URL https://news.un.org/en/story/2021/08/1097362.
[2] D. Sadeghi, S.E. Ahmadi, N. Amiri, Satinder, M. Marzband, A. Abusorrah, M. Rawa, Designing, optimizing and comparing distributed generation technologies as a substitute system for reducing life cycle costs, CO2 emissions, and power losses in residential buildings, Energy 253 (2022) 123947.
[3] M.D. Ilić, P.M. Carvalho, From hierarchical control to flexible interactive electricity services: A path to decarbonisation, Electr. Power Syst. Res. 212 (2022) 108554.
[4] A. Komarova, I. Filimonova, A. Kartashevich, Energy consumption of the countries in the context of economic development and energy transition, Energy Rep. 8 (2022) 683–690.
[5] M.D. Dean, K.M. Kockelman, Are electric vehicle targets enough? The decarbonization benefits of managed charging and second-life battery uses, Transp. Res. Rec. 2676 (8) (2022) 24–43.
[6] A. Azarhooshang, D. Sedighizadeh, M. Sedighizadeh, Two-stage stochastic operation considering day-ahead and real-time scheduling of microgrids with high renewable energy sources and electric vehicles based on multi-layer energy management system, Electr. Power Syst. Res. 201 (2021) 107527.
[7] Y. Dong, F. Liu, X. Lu, Y. Lou, Y. Ma, N. Eghbalian, Multi-objective economic environmental energy management microgrid using hybrid energy storage implementing and developed manta ray foraging optimization algorithm, Electr. Power Syst. Res. 211 (2022) 108181.
[8] F. Ahmad, A. Iqbal, I. Ashraf, M. Marzband, I. khan, Optimal location of electric vehicle charging station and its impact on distribution network: A review, Energy Rep. 8 (2022) 2314–2333.
[9] Trends in life cycle greenhouse gas emissions of future light duty electric vehicles, Transp. Res. D 81 (2020) 102287.
[10] Y. Ma, T. Shi, W. Zhang, Y. Hao, J. Huang, Y. Lin, Comprehensive policy evaluation of NEV development in China, Japan, the United States, and Germany based on the AHP-EW model, J. Clean. Prod. 214 (2019) 389–402.
[11] R. Zhang, J. Zhang, Y. Long, W. Wu, J. Liu, Y. Jiang, Long-term implications of electric vehicle penetration in urban decarbonization scenarios: An integrated land use–transport–energy model, Sustainable Cities Soc. 68 (2021) 102800.
[12] E. Fouladi, H.R. Baghaee, M. Bagheri, G.B. Gharehpetian, Power management of microgrids including PHEVs based on maximum employment of renewable energy resources, IEEE Trans. Ind. Appl. 56 (5) (2020) 5299–5307.
[13] H. Mehrjerdi, Off-grid solar powered charging station for electric and hydrogen vehicles including fuel cell and hydrogen storage, Int. J. Hydrogen Energy 44 (23) (2019) 11574–11583.
[14] A. Modarresi Ghazvini, J. Olamaei, Optimal sizing of autonomous hybrid PV system with considerations for V2G parking lot as controllable load based on a heuristic optimization algorithm, Sol. Energy 184 (2019) 30–39.
[15] M.R. Mozafar, M.H. Amini, M.H. Moradi, Innovative appraisement of smart grid operation considering large-scale integration of electric vehicles enabling V2G and G2V systems, Electr. Power Syst. Res. 154 (2018) 245–256.
[16] S. Wang, Z.Y. Dong, F. Luo, K. Meng, Y. Zhang, Stochastic collaborative planning of electric vehicle charging stations and power distribution system, IEEE Trans. Ind. Inform. 14 (1) (2018) 321–331.
[17] J. Zhong, X. Xiong, An orderly EV charging scheduling method based on deep learning in cloud-edge collaborative environment, Artif. Intell. Internet Things (IoT) Civ. Eng. (2021) 1–19.
[18] R. Das, Y. Wang, G. Putrus, R. Kotter, M. Marzband, B. Herteleer, J. Warmerdam, Multi-objective techno-economic-environmental optimisation of electric vehicle for energy services, Appl. Energy 257 (2020) 113965.
[19] M.J. Morshed, J.B. Hmida, A. Fekih, A probabilistic multi-objective approach for power flow optimization in hybrid wind-PV-PEV systems, Appl. Energy 211 (2018) 1136–1149.
[20] M. Tostado-Véliz, S. Kamel, H.M. Hasanien, R.A. Turky, F. Jurado, Optimal energy management of cooperative energy communities considering flexible demand, storage and vehicle-to-grid under uncertainties, Sustainable Cities Soc. 84 (2022) 104019.
[21] C. Liu, S.S. Abdulkareem, A. Rezvani, S. Samad, N. Aljojo, L.K. Foong, K. Nishihara, Stochastic scheduling of a renewable-based microgrid in the presence of electric vehicles using modified harmony search algorithm with control policies, Sustainable Cities Soc. 59 (2020) 102183.
[22] H. Ganjeh Ganjehlou, H. Niaei, A. Jafari, D.O. Aroko, M. Marzband, T. Fernando, A novel techno-economic multi-level optimization in home-microgrids with coalition formation capability, Sustainable Cities Soc. 60 (2020) 102241.

[23] T. Rawat, K. Niazi, N. Gupta, S. Sharma, Multi-objective techno-economic operation of smart distribution network integrated with reactive power support of battery storage systems, Sustainable Cities Soc. 75 (2021) 103359.
[24] A.K. Barik, D.C. Das, Integrated resource planning in sustainable energy-based distributed microgrids, Sustain. Energy Technol. Assess. 48 (2021) 101622.
[25] A. Mansour-Saatloo, R. Ebadi, M.A. Mirzaei, K. Zare, B. Mohammadi-Ivatloo, M. Marzband, A. Anvari-Moghaddam, Multi-objective IGDT-based scheduling of low-carbon multi-energy microgrids integrated with hydrogen refueling stations and electric vehicle parking lots, Sustainable Cities Soc. 74 (2021) 103197.
[26] M. Shamshirband, J. Salehi, F.S. Gazijahani, Decentralized trading of plug-in electric vehicle aggregation agents for optimal energy management of smart renewable penetrated microgrids with the aim of CO2 emission reduction, J. Clean. Prod. 200 (2018) 622–640.
[27] K. Gholami, S. Karimi, A. Anvari-Moghaddam, Multi-objective stochastic planning of electric vehicle charging stations in unbalanced distribution networks supported by smart photovoltaic inverters, Sustainable Cities Soc. 84 (2022) 104029.
[28] M.J. Mayer, A. Szilágyi, G. Gróf, Environmental and economic multi-objective optimization of a household level hybrid renewable energy system by genetic algorithm, Appl. Energy 269 (2020) 115058.
[29] S.E. Ahmadi, D. Sadeghi, M. Marzband, A. Abusorrah, K. Sedraoui, Decentralized bi-level stochastic optimization approach for multi-agent multi-energy networked micro-grids with multi-energy storage technologies, Energy 245 (2022) 123223.
[30] W. Römisch, Scenario reduction techniques in stochastic programming, in: O. Watanabe, T. Zeugmann (Eds.), Stochastic Algorithms: Foundations and Applications, Springer, Berlin, Heidelberg, 2009, pp. 1–14.
[31] X.-S. Yang, M. Karamanoglu, 1 - swarm intelligence and bio-inspired computation: An overview, in: X.-S. Yang, Z. Cui, R. Xiao, A.H. Gandomi, M. Karamanoglu (Eds.), Swarm Intelligence and Bio-Inspired Computation, Elsevier, Oxford, 2013, pp. 3–23.
[32] O. Ivanov, B.-C. Neagu, G. Grigoras, M. Gavrilas, Optimal capacitor bank allocation in electricity distribution networks using metaheuristic algorithms, Energies 628 (22) (2016) 62–68.
[33] S.E. Ahmadi, N. Rezaei, An IGDT-based robust optimization model for optimal operational planning of cooperative microgrid clusters: A normal boundary intersection multi-objective approach, Int. J. Electr. Power Energy Syst. 127 (2021) 106634.
[34] S. Katiyar, R. Patel, K. Arora, Comparison and analysis of cuckoo search and firefly algorithm for image enhancement, Smart Trends Inf. Technol. Comput. Commun. 12 (22) (2019).
[35] S.E. Ahmadi, N. Rezaei, A new isolated renewable based multi microgrid optimal energy management system considering uncertainty and demand response, Int. J. Electr. Power Energy Syst. 118 (2020) 105760.
[36] J. Wang, B. Yang, D. Li, C. Zeng, Y. Chen, Z. Guo, X. Zhang, T. Tan, H. Shu, T. Yu, Photovoltaic cell parameter estimation based on improved equilibrium optimizer algorithm, Energy Convers. Manage. 236 (2021) 114051.
[37] H. Zheng, W. Huang, J. Zhao, J. Liu, Y. Zhang, Z. Shi, C. Zhang, A novel falling model for wind speed probability distribution of wind farms, Renew. Energy 184 (2022) 91–99.
[38] V.E. Duca, T.C. Fonseca, F.L. Cyrino Oliveira, A generalized dynamical model for wind speed forecasting, Renew. Sustain. Energy Rev. 136 (2021) 110421.
[39] S.E. Ahmadi, N. Rezaei, H. Khayyam, Energy management system of networked microgrids through optimal reliability-oriented day-ahead self-healing scheduling, Sustain. Energy Grids Netw. 23 (2020) 100387.
[40] D. Li, Y. Li, Z. Ma, M. Zheng, Z. Lu, Exergetic performance coefficient analysis and optimization of a high-temperature proton exchange membrane fuel cell, Membranes 12 (1) (2022).
[41] S.R. Fahim, H.M. Hasanien, R.A. Turky, A. Alkuhayli, A.A. Al-Shamma'a, A.M. Noman, M. Tostado-Véliz, F. Jurado, Parameter identification of proton exchange membrane fuel cell based on hunger games search algorithm, Energies 14 (16) (2021).
[42] S.E. Ahmadi, M. Marzband, A. Ikpehai, A. Abusorrah, Optimal stochastic scheduling of plug-in electric vehicles as mobile energy storage systems for resilience enhancement of multi-agent multi-energy networked microgrids, J. Energy Storage (2022).
[43] L. Bagherzadeh, H. Shayeghi, S. Pirouzi, M. Shafie-khah, J.P.S. Catalão, Coordinated flexible energy and self-healing management according to the multi-agent system-based restoration scheme in active distribution network, IET Renew. Power Gener. 15 (8) (2021) 1765–1777.
[44] A. Zakariazadeh, S. Jadid, P. Siano, Multi-objective scheduling of electric vehicles in smart distribution system, Energy Convers. Manage. 79 (2014) 43–53.